Drug resistance by evasion of antiangiogenic targeting of VEGF signaling in late-stage pancreatic islet tumors

Oriol Casanovas,[1] Daniel J. Hicklin,[2] Gabriele Bergers,[3] and Douglas Hanahan[1,*]

[1]Department of Biochemistry and Biophysics, Comprehensive Cancer Center, and Diabetes Center, University of California, San Francisco, San Francisco, California 94143
[2]ImClone Systems Inc., New York, New York 10014
[3]Brain Tumor Research Center and Department of Neurosurgery, University of California, San Francisco, San Francisco, California 94143
*Correspondence: dh@biochem.ucsf.edu

Summary

Function-blocking antibodies to VEGF receptors R1 and R2 were used to probe their roles in controlling angiogenesis in a mouse model of pancreatic islet carcinogenesis. Inhibition of VEGFR2 but not VEGFR1 markedly disrupted angiogenic switching, persistent angiogenesis, and initial tumor growth. In late-stage tumors, phenotypic resistance to VEGFR2 blockade emerged, as tumors regrew during treatment after an initial period of growth suppression. This resistance to VEGF blockade involves reactivation of tumor angiogenesis, independent of VEGF and associated with hypoxia-mediated induction of other proangiogenic factors, including members of the FGF family. These other proangiogenic signals are functionally implicated in the revascularization and regrowth of tumors in the evasion phase, as FGF blockade impairs progression in the face of VEGF inhibition.

Introduction

Tumor angiogenesis is regulated by a balance of pro- and antiangiogenic molecules, and when the balance shifts in favor of angiogenesis inducers, an angiogenic switch activates the normally quiescent vasculature to develop new blood vessels (Hanahan and Folkman, 1996), often concomitant with enlargement (dilation and microhemorrhaging) of the preexisting vasculature (Ryschich et al., 2002). A prominent proangiogenic signaling circuit involves the vascular endothelial growth factor (VEGF) family, and in particular VEGF-A (Ferrara et al., 2003). VEGF ligands bind to two transmembrane tyrosine kinase receptors expressed in blood vessel endothelial cells: VEGF receptor 1 (VEGFR1, Flt-1) and VEGF receptor 2 (VEGFR2, KDR in humans, Flk1 in mice) (Shibuya, 2001). A number of clinical trials are underway to test the utility of anti-VEGF or anti-VEGFR therapies in a variety of cancers (Angiogenesis Inhibitors in Clinical Trials, National Cancer Institute, http://www.cancer.gov/clinicaltrials/developments/anti-angio-table/). A recent phase III clinical trial demonstrated that bevacizumab (Avastin), a humanized monoclonal antibody against VEGF-A, in combination with conventional chemotherapy, increased overall survival by 5 months in colorectal cancer patients (Hurwitz et al., 2004), leading to FDA approval. Much as for other therapeutic strategies, apparent resistance to antiangiogenic therapies has been described in clinical trials and in xenotransplant tumor models (Kerbel et al., 2001; Miller et al., 2003, 2005); in particular, the development of nonresponsiveness to an initially efficacious anti-VEGFR therapeutic regimen in a xenotransplant model has been documented (Klement et al., 2000), by an unknown mechanism.

Here, we use specific function-blocking monoclonal antibodies to two VEGF receptors to probe their role in mediating and sustaining angiogenesis and tumor growth in an endogenous mouse model of islet cell carcinogenesis, where the functional importance of VEGF signaling has been previously documented, via gene knockout of VEGF-A (Inoue et al., 2002) and pharmacological inhibition of VEGF receptors with small molecules (Bergers et al., 2000, 2003). The results presented herein demonstrate that VEGFR2 is necessary for the angiogenic switch and for sustaining tumor angiogenesis but in addition document the emergence of phenotypic resistance to the VEGFR2 blockade that allows for revascularization and regrowth of treated tumors.

SIGNIFICANCE

Numerous clinical trials are testing the efficacy of anti-VEGF/VEGF receptor therapies for various cancers. Several phase III trials have provided evidence that anti-VEGF therapy, alone or in combination with chemotherapy, is efficacious and produces a transitory stable disease followed by progression in several types of cancer. Here, we describe a mouse model of cancer wherein VEGFR2 inhibition also produces a period of stable disease followed by progression. We show that phenotypic resistance emerges to anti-VEGFR2 therapy, which may explain the inevitable progression; this resistance involves vascular regrowth in a VEGF-independent second wave of angiogenesis, mediated in part by proangiogenic ligands of the FGF family. Counteracting such mechanisms of resistance by multitargeting alternative proangiogenic signaling circuits may improve efficacy of antiangiogenic therapies.

Results

Immunodeficient islet cell carcinogenesis model

Our experimental design aimed to use rat monoclonal antibodies that block ligand binding and consequent signaling by VEGFR2 (MAb DC101) and VEGFR1 (MAb MF1) in the RIP-Tag2 mouse model of islet cell carcinogenesis to probe receptor functions and relative importance. To avoid the confounding biases of neutralizing antibody responses, we developed an immunodeficient variant of this prototypical model of cancer, by rendering it homozygous deficient for the recombinase activator gene 1 (Rag1). Mice lacking Rag1 are unable to perform V(D)J recombination of immunoglobulins and T cell receptor genes during immune cell maturation, and thus are completely deficient in adaptive immunity (Mombaerts et al., 1992). We first characterized the tumorigenesis phenotype in *RIP1-Tag2, Rag1*$^{-/-}$ mice, which revealed the same multistage tumor progression, with no apparent change in the histological phenotype of the tumors (Figure S1 in the Supplemental Data available with this article online). At end stage (13.5 weeks of age), the immunodeficient animals showed similar tumor burden (102 ± 23 mm^3 compared to 110 ± 36 mm^3 in immunocompetent controls), similar tumor number (7 ± 2 tumors in immunodeficient animals compared to 8 ± 4 in immunocompetent controls), and no change in the inflammatory infiltration of innate immune cells, such as macrophages and granulocytes (Figure S1 and data not shown). In contrast to the characteristic presence of macrophages and neutrophils in premalignant and malignant lesions, infiltration of mature B or T cells in the tumors is not evident in the wild-type (immunocompetent) RIP1-Tag2 mice (unpublished data), and indeed RIP-Tag2 mice are evidently self tolerant of their tumors (Adams et al., 1987; Jolicoeur et al., 1994). The current analysis of the *RIP1-Tag2, Rag1*$^{-/-}$ mice extends upon these previous studies, demonstrating that mature B and T lymphocytes cannot be factors in pancreatic islet tumorigenesis in RIP-Tag2 mice, either as enhancers or antagonists, since their absence neither attenuates nor accelerates tumorigenesis, in contrast, for example, to mouse models of skin cancer and cervical cancer, where the adaptive immune system either promotes (Daniel et al., 2003; de Visser et al., 2005) or antagonizes (Daniel et al., 2005) tumorigenesis.

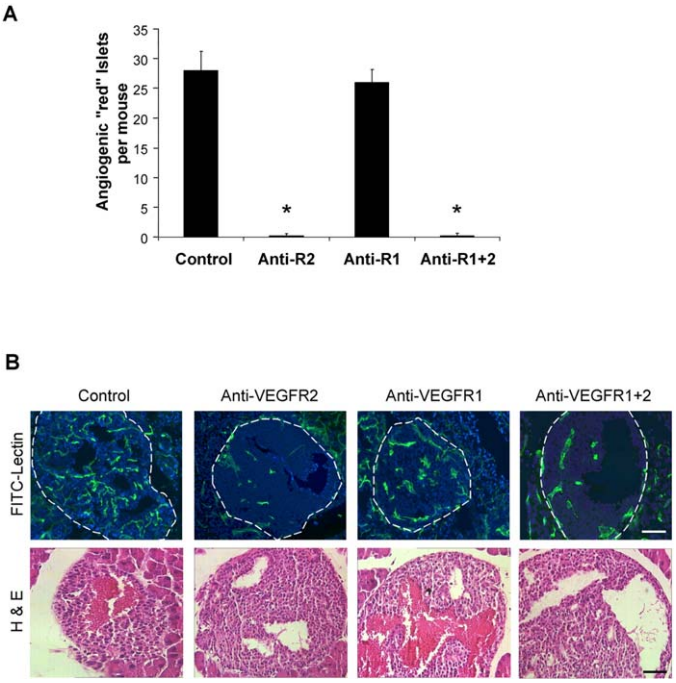

Figure 1. Antibody blockade of VEGFR2 but not VEGFR1 impairs angiogenesis in pancreatic islet dysplasias, decreasing vessel density and microhemorrhaging

A: Quantification of number of angiogenic "red" islets per animal in the different arms of treatment: control IgG, VEGFR2-blocking antibody, VEGFR1-blocking antibody, and the combination of both VEGFR-blocking antibodies. Averages of number of angiogenic islets per animal in cohorts of eight to ten mice per arm are shown with their respective standard deviation bars. *Statistically significant using Mann-Whitney test ($p < 0.02$) when compared to control group.

B: Visualization of the vessels and histologic analysis of the microhemorrhaging in the treated and nontreated islet dysplasias. Vessels were labeled by i.v. perfusion of FITC-conjugated tomato lectin (green) followed by DAPI counterstaining (blue), and neoplastic islets are delineated with a white dotted line; hematoxylin and eosin (H&E) staining shows the microhemorrhaged erythrocytes that have markedly accumulated in the core of the islets, or not in the case of the anti-VEGFR2-treated animals. Representative images are shown from an analysis of five sections per animal from a minimum of five mice per group; scale bar, 50 μm.

VEGFR2 blockade impairs angiogenesis and tumorigenesis

The well-documented and relatively synchronous angiogenic switching and multistage tumorigenesis in the RIP-Tag2 mouse model of cancer allows for testing experimental therapies in three "trial designs" that variously (1) assess effects on angiogenic switching in progenitor lesions (prevention trial), (2) score the explosive growth of nascent solid tumors (intervention trial), or (3) ask whether tumor burden can be reduced or stabilized concomitant with life span extension (regression trial) (Bergers et al., 1999, 2000, 2003).

To evaluate the effects of VEGFR-blocking antibodies on the angiogenic switch that first activates angiogenesis, we initiated treatment of animals at 5 weeks of age (before the angiogenic switch) and continued treatment for 3 weeks. While in mock-treated animals the angiogenic switch resulted in hypervascularized "red islets" with a dilated, microhemorrhaging vasculature, VEGFR2 blockade produced a significant decrease in angiogenesis and abolished the appearance of red islets (Figure 1A). In contrast, VEGFR1 blockade did not have a discernible effect. Histological analysis showed that VEGFR2-blocking treatment significantly reduced vessel density, as shown by systemic perfusion with a fluorescently labeled tomato lectin, and impaired the characteristic microhemorrhaging as seen by accumulation of erythrocytes inside the islets (previously described as blood islands) (Figure 1B). We next asked whether simultaneous blockade of VEGFR1 and -2 would further inhibit angiogenesis above and beyond VEGFR2 inhibition alone. The data show that blocking both receptors did not significantly improve upon the antiangiogenic effects of VEGFR2 blockage (Figure 1). These results are consistent with the well-established importance of VEGF as a proangiogenic and vascular permeability factor and reveal that VEGFR2 but not VEGFR1 is crucial for the angiogenic switch in this tumor model. Given previous work demonstrating that infiltrating inflammatory cells

are critical in supplying matrix metalloproteinases necessary to trigger the angiogenic switch (Bergers et al., 2000), and the report that certain inflammatory cells (i.e., macrophages) can utilize the VEGF/VEGFR1 pathway for chemotaxis (Sawano et al., 2001), we asked if VEGFR1 blockade was affecting the mobilization and infiltration of these cells into the tumors. Immunostaining with several macrophage markers indicated that macrophage infiltration was not affected by blocking VEGFR1, suggesting that other signaling pathways mediate the recruitment of these cells into the islet tumors (data not shown).

Given that VEGFR1 is expressed in both the premalignant and tumor stages in this model (Christofori et al., 1995; and data not shown), the marked ineffectiveness of the VEGFR1 antibody in all of our experiments led us to reconfirm its functional activity. We tested the functional activity of MF1 in blocking VEGFR1 function in a previously validated in vivo assay where VEGFR1 is demonstrably important (Passaniti et al., 1992). In this assay, we treated animals with implanted subcutaneous matrigel plugs with the same dosage regimen of VEGFR1-blocking antibody used in RIP-Tag2 animals, assessing neovascularization of the VEGF-containing plug. The results showed that MF1 was active and able to block VEGFR1 function in vivo in the same dosage regimen (Figure S2), consistent with a previous study (Luttun et al., 2002).

To evaluate the effects of the selective VEGFR1/2-blocking antibodies on tumor formation and tumor growth subsequent to the angiogenic switch, we initiated treatment in 10-week-old animals, before the appearance of tumors, and continued the treatment until 13.5 weeks of age, when end-stage tumors are present. In this regimen, VEGFR2 blockade produced a significant impairment of tumor formation, while blockade of VEGFR1 had no effect (Figure 2A). Treatment with VEGFR2-blocking antibodies significantly reduced the accumulated tumor burden per animal (by 50%). The impaired tumor growth was associated with clear histopathological differences in the treated tumors, which evidenced marked decreases in vessel density, vascular dilation, and permeability/microhemorrhaging (Figure 2B). In contrast, VEGFR1 blockade with MF1 had no effect (Figure 2A and data not shown). Notably, there was a proportional decrease in tumor burden compared to vessel density and vascular permeability in response to anti-VEGFR2 (Figures 2A and 2B), suggesting a causal link between these parameters. We asked whether simultaneous blockade of VEGFR1 and VEGFR2 would further inhibit angiogenesis and tumor growth compared to VEGFR2 inhibition alone. Blocking both receptors did not significantly improve upon the antiangiogenic and antitumor effects of VEGFR2 inhibition alone (Figure 2 and data not shown).

Surprisingly, although the tumors were smaller in the mice receiving the VEGFR2-blocking treatment, the tumors had a significantly more invasive and malignant phenotype; most had wide fronts of invasion into the surrounding acinar tissue (Figure 2C). This more invasive phenotype was even more striking following immunostaining for the tumor's collagenous capsule with collagen I antibody. As shown in Figure 2C, mock-treated tumors had a thick collagenous capsule that delineated them from the surrounding acinar tissue, while the anti-VEGFR2-treated tumors had a much thinner capsule with areas of breakage or completely absent capsule. Increased invasiveness consequent to antiangiogenic therapies, including kinase inhibitors targeting VEGF receptors, has been observed in previous studies in this model (Bergers et al., 1999, 2000), as well as in other models of cancer (Pennacchietti et al., 2003; Steeg, 2003).

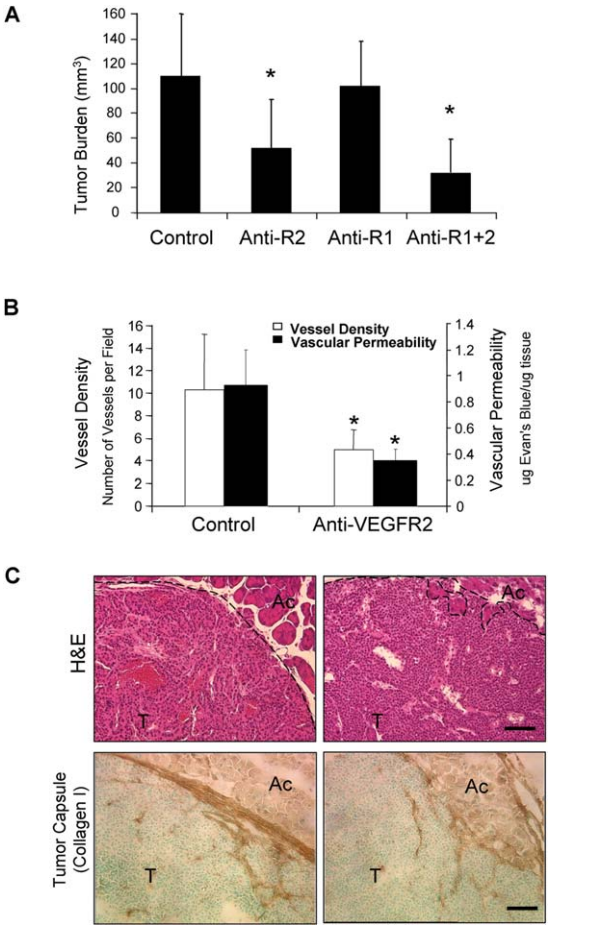

Figure 2. VEGFR2-blocking antibody treatment selectively inhibits tumorigenesis, with decreased vessel density and vascular permeability

A: Total tumor burden per animal is plotted for the different treatment arms, each involving cohorts of eight to ten mice per group, with their respective standard deviation bars. *Statistically significant using Mann-Whitney test ($p < 0.02$) when compared to control group.

B: Quantification of intratumoral vessel density (white bars, left axis) and vascular permeability analysis by Miles assay (black bars, right axis) with their standard deviation bars. *Statistically significant differences were found between VEGFR2-blocking treatment and control cohorts in both analyses using the Mann-Whitney test ($p < 0.02$).

C: Histological images of tumors by H&E staining, and by collagen I immunohistochemistry to visualize the tumor capsule (brown). Representative images are shown from an analysis of five sections per animal from a minimum of five mice per group. T, tumor; Ac, surrounding acinar tissue; scale bar, 50 μm. Tumors treated with anti-R1 were similar to controls by all criteria, and the combination anti-R1 + R2 treatment was comparable to anti-R2 alone (data not shown).

Surprising regrowth of established tumors under VEGFR2-blocking treatment

To evaluate the capability of the VEGFR-blocking antibodies to stabilize or regress late-stage tumors and extend life span, we initiated treatment on 12-week-old animals, when there is al-

ready a significant accumulated tumor burden (60 mm^3). Initially, cohorts of eight to ten mice were treated for 10 days beginning at 12 weeks of age, until the mock-treated controls had reached end stage (13.5 weeks). As shown in Figure 3A, mock-treated animals approximately doubled their tumor burden during this time of treatment, whereas VEGFR2-blocking treatment stabilized the tumor burden, producing a 50% reduction in accumulated tumor burden after the 10 days of treatment compared to the control cohort. Once again, VEGFR1 blockade did not show any difference compared to controls, and the combination of anti-VEGFR1 and anti-VEGFR2 did not further enhance the VEGFR2-blocking antibody's effects (Figure 3A). Fluorescent-lectin perfusion of the tumor vasculature revealed a significantly reduced vessel density in the VEGFR2-treated animals with stable tumor burden, in comparison with the other cohorts where tumors grew during this period (Figure 3B and data not shown). The data indicate that, during this short time of treatment, VEGFR2 blockade was targeting the angiogenic tumor vasculature and consequently restraining tumor growth.

We next sought to extend the treatment for a total period of 4 weeks, well after the control animals died of their tumor burden, in a standard regression trial (according to Bergers et al., 1999, 2003). In this regimen, VEGFR2 blockade produced a modest survival benefit, in that all treated mice lived to the defined endpoint of +4 weeks. Analysis of tumor burden, however, revealed that the initial "stable disease" phase was followed by progression, a surprising regrowth of the anti-VEGFR2-treated tumors (Figure 3A). This regrowth phase led to an accumulated tumor burden per animal that was comparable to that found in end-stage control animals. Again, there was no added benefit from combining the anti-VEGFR1 and anti-VEGFR2. In both cohorts (blocking VEGFR2 only, or R1 + R2), the tumors that grew during the extended treatment showed a more invasive and malignant phenotype (data not shown). In regard to the vasculature, two distinctive classes were apparent in the regrowth phase, as revealed by vascular perfusion. The predominant class had increased vascular density and the biomarkers of angiogenesis (dilated vessels, microhemorrhaging), comparable to untreated tumors, and were markedly distinct from the tumors in the transitory stable disease phase (at +10 days) (compare Figure 3Bd with Figure 3Be). Additionally, we observed a rare class of tumors that did not evidence an increased vascular density but rather contained small vessels with less branching at their periphery (marked by arrowheads in Figure 3Bf). These more "normal" vessels are typical of those observed in the normal exocrine pancreas. A similar histological pattern of vascularization has been reported in other tumor models as well as in certain human tumors and has been termed "vessel cooption" of the adjacent "normal" vasculature by neoplasms (Holash et al., 1999; Leenders et al., 2004; Pezzella et al., 1997). Rebounding tumors with apparent coopted vessels and no evident angiogenesis were rare, and thus have not been included in the subsequent molecular analysis of the revascularization. To quantitatively assess the extent of revascularization that occurred in the majority class of tumors in the relapse phase, vessel density analysis was performed at various time points during the anti-VEGFR2-blocking treatment. As shown in Figure 3C, the short 10 day treatment produced a statistically significant decrease in vessel density, whereas upon extending the treatment for a total of 4 weeks, the vessel

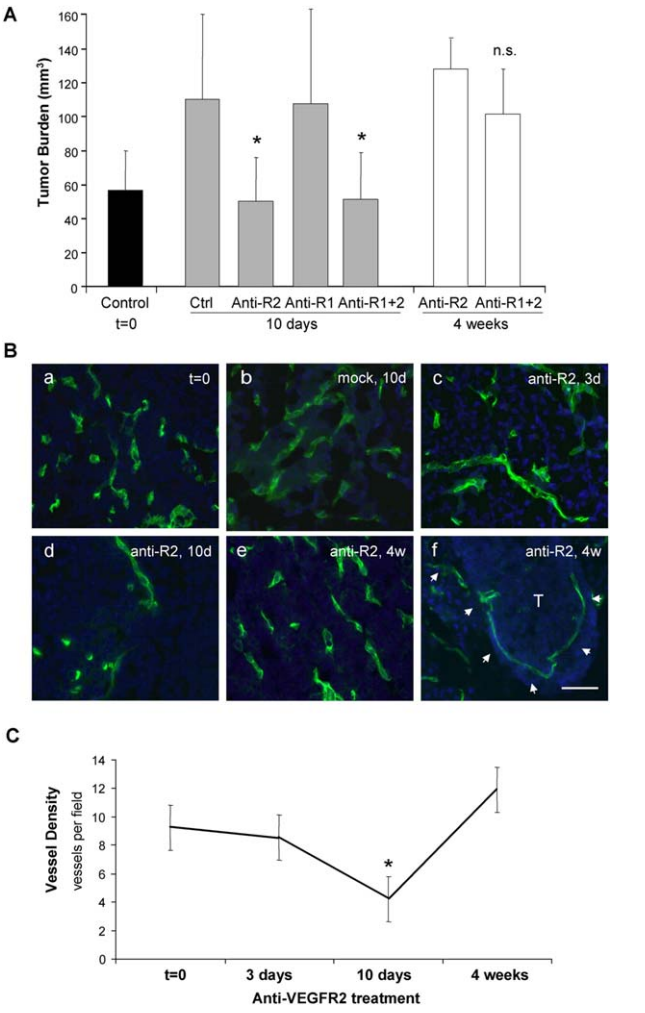

Figure 3. VEGFR2 blockade transiently stops tumor growth and decreases vascularity, followed by tumor progression, reinduction of angiogenesis, and reestablishment of the tumor vasculature

A: Quantification of overall tumor burden plotted as average and standard deviation per animal at the time of initiation of treatment (t = 0; black bar) and after treatment for 10 days (gray bars) and for 4 weeks of age (white bars) for the different treatment arms. Averages from cohorts of eight to ten mice per group are plotted with their respective standard deviation bars. *Statistically significant differences using Mann-Whitney test ($p < 0.02$) compared to age-matched controls.

B: Vessel labeling by FITC-conjugated tomato lectin (green) and DAPI counterstain of nuclei (blue) from nontreated animals (**Ba**); animals that received mock treatment for 10 days (**Bb**); or animals that were treated with anti-VEGFR2 antibodies for 3 days (**Bc**), for 10 days (**Bd**), or for 4 weeks showing revascularization (**Be**), or for 4 weeks showing cooption (**Bf**). Images shown are representative of a total of five sections per animal from a minimum of five mice per group analyzed. Tumors are marked as "T." White arrowheads in **Bf** point to a normal vessel that runs along the tissue boundary and is possibly coopted by the growing tumor. Scale bar, 50 μm.

C: Quantification of the vessel density in the anti-VEGFR2-treated tumors at 3 days, 10 days, and 4 weeks of treatment compared to t = 0 controls. Averages from a minimum of eight images corresponding to four to five mice per time point are plotted with their respective standard deviation bars. *Statistically significant decrease compared to controls using the Mann-Whitney test ($p < 0.01$).

density returned to higher levels, comparable to that in untreated tumors. These results suggest that, concomitant with the reinitiation of tumor growth in the extended treatment, angiogenesis is reactivated and the vessel density is reestablished. Thus, the initial vascular disruption caused by the VEGFR2-blocking treatment is evidently followed by a second wave of angiogenesis in most tumors that is capable of reestablishing a typically dense and aberrant tumor vasculature. This result suggests the emergence of resistance to or evasion of the VEGF blockage by the tumor endothelium.

To address one possible explanation, that the blocking antibody was losing effectiveness in the long-term treatment, we analyzed the tumors from the extended anti-VEGFR2 treatment for phenotypic and molecular markers of the VEGFR2 inhibition, such as microhemorrhaging, vascular permeability, and the phosphorylation status of VEGFR2. While the control mock-treated tumors showed the apparent microhemorrhaging and redness typical of the islet tumors in these mice, the long-term anti-VEGFR2-treated tumors still showed a white non-hemorrhaging phenotype (Figure 4A), which is consistent with our results in earlier-stage intervention and short regression trials (data not shown) and is in accordance with the inhibition of VEGFR2's vascular permeability function. Furthermore, to assess the molecular efficacy of the anti-VEGFR2 blockade of receptor signaling, the phosphorylation status of VEGFR2 in the treated tumors was determined using antibodies that are diagnostic of VEGFR2 activation, by recognizing a phosphorylation site in the VEGFR2 kinase domain, of tyrosine 951 (Y951) (Dougher-Vermazen et al., 1994; Matsumoto et al., 2005). As shown in Figure 4B, VEGFR2 phosphorylation of Y951 was readily detected in tumors from control, mock-treated animals by Western blotting, but not in the 10 day responding or the 4 week rebounding tumors being treated with anti-VEGFR2 antibody. Quantification of phospho-VEGFR2 in treated tumors compared to controls showed a >90% reduction in detectable receptor phosphorylation in tumors from the anti-VEGFR2-treated animals, which is statistically significant ($p > 0.02$) using the Mann-Whitney U test. Thus, both the maintained lack of microhemorrhaging and redness and the molecular analysis of VEGFR2 phosphorylation demonstrate that the VEGFR2-blocking antibody retains its functional activity in inhibiting the signaling by its target receptor throughout the 4 weeks of treatment, despite its only transitory capability to stop tumor growth and reduce tumor vascularity.

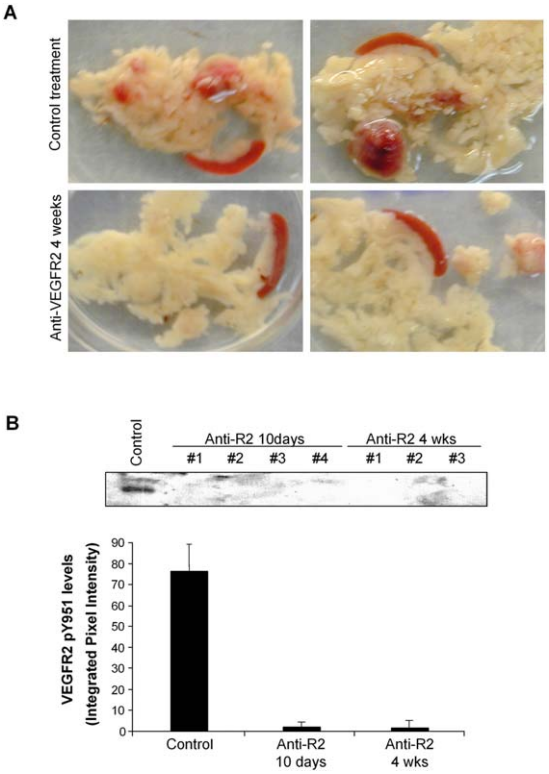

Figure 4. Continuing molecular efficacy of the VEGFR2-blocking antibody during the phenotypic evasion phase

A: Gross pathology images of the excised pancreas and spleen from animals after 4 weeks of treatment showing the "red" vascularized and hemorrhaging phenotype of the control tumors, and lack thereof in the 4 week anti-VEGFR2-treated tumors due to continued blocking of VEGFR2.

B: VEGFR2 phosphorylation status detected by Western blot from whole tumors using an antibody that specifically recognizes phospho-Y951 of VEGFR2. Phosphorylation in Y951 was detected in tumors from mock-treated animals (Control) but is absent in the tumors treated with anti-VEGFR2 for 10 days or 4 weeks. Quantification of phospho-Y951-VEGFR2 in treated tumors compared to controls is shown as a bar graph of average band intensity with standard deviation bars. Both short and long treatment with anti-VEGFR2 antibody show a >90% reduction in detectable receptor phosphorylation, which is statistically significant ($p > 0.01$) using the Mann-Whitney U test.

Short-term VEGFR2 blockade triggers hypoxia and upregulation of other proangiogenic factors

To begin investigating the mechanism of this apparent evasion of VEGFR2 blockade, we evaluated possible changes in the microenvironment of the tumors that could be triggered by the VEGFR2 blockade. One possible factor was hypoxia, as it has been described that a variety of angiogenesis inhibitors can trigger hypoxia in treated tumors (Yu et al., 2002). Indeed, we found that short-term anti-VEGFR2-treated tumors had clear areas of hypoxia, as detected by formation of pimonidazole adducts and by detection of the hypoxia-regulated transcription factor HIF-1α, effects that were undetectable in the untreated tumors (Figure 5A and data not shown). Surprisingly, the acute hypoxia visualized by pimonidazole was transitory, being detectable only in the tumors after the short-term (10 day) anti-VEGFR2 treatment, but not in the longer-term (4 week) treatment; we infer that the revascularization (or in rare cases normal vessel cooption) had ameliorated the acute hypoxia.

Hypoxia is a known inducer of angiogenic responses in a wide variety of tumor types, involving induction of gene expression, via the HIF transcription factor, of various proangiogenic factors, including VEGF and FGFs (reviewed in Pugh and Ratcliffe, 2003). This knowledge motivated a candidate gene expression profiling analysis, by Q-RT-PCR (TaqMan) on mRNA from total tumors, to assess possible changes in a set of proangiogenic factors, including ones previously implicated in RIP-Tag2 angiogenesis, namely FGFs and Ephrins (Brantley et al., 2002; Cheng et al., 2003; Compagni et al., 2000). This analysis revealed that several members of the FGF, Ephrin, and Angiopoietin families of proangiogenic factors were upregulated in the context of VEGFR2-blocking treatment when compared to mock-treated controls (Figure 5B). In particular,

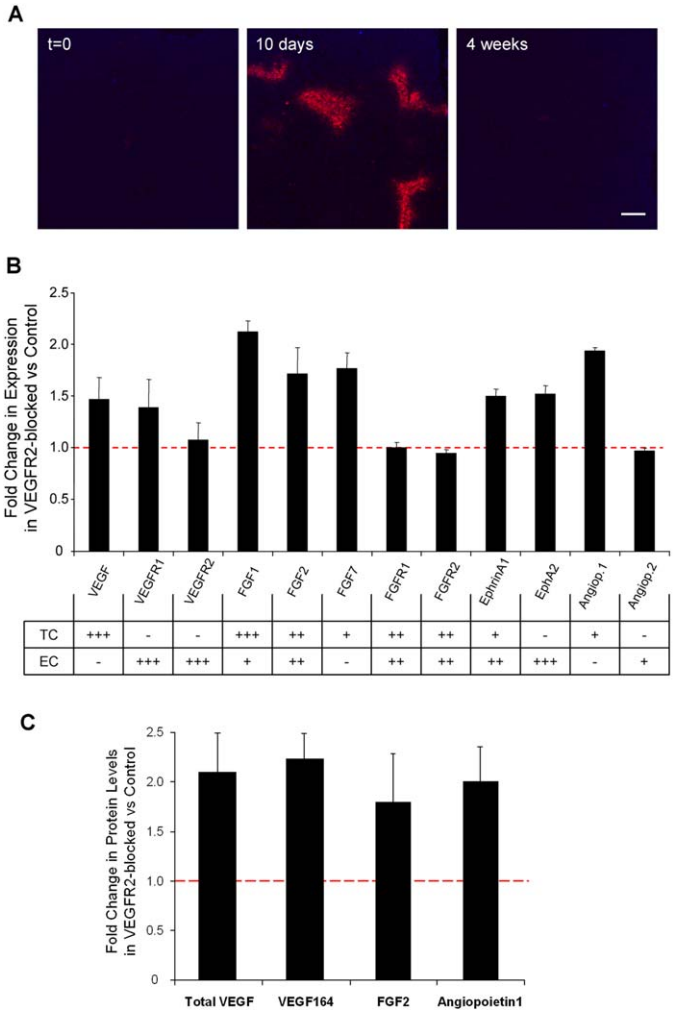

Figure 5. Short-term VEGFR2 blockade promotes hypoxia and a change in the expression of proangiogenic factors in tumors

A: Hypoxia in islet tumors was detected by the formation of pimonidazole adducts as described in the Experimental Procedures. Immunodetection of pimonidazole adducts is shown in red, and nuclei counterstained with DAPI are shown in blue. Images shown are representative of an analysis of a minimum of five sections from each of three animals at t = 0, t = 10 days, or t = 4 weeks of anti-VEGFR2-blocking treatment; scale bar, 50 μm.

B: Quantitative RT-PCR expression analysis of different proangiogenic factors and their primary receptors in total tumors from the anti-VEGFR2-treated tumors compared to control tumors. Bar graph shows fold upregulation of each molecule in VEGFR2-blocking treatment comparing to controls. Values represent averages and standard deviations of two independent experiments, and the red dotted line represents a value of 1 (no change of expression in treatment). The boxes underneath indicate the presence (+) or absence (−) and relative abundance of each molecule's mRNA expression in FACS-sorted cell populations from the tumors (TC, tumor cell compartment; EC, endothelial cell compartment) as determined by quantitative RT-PCR.

C: Analysis of protein levels of different proangiogenic factors in total tumors from the anti-VEGFR2-treated tumors compared to control tumors, by Western blot (VEGF-164 and Angiopoietin-1) or by ELISA-based commercial antibody array (total VEGF and FGF2). Bar graph shows fold upregulation of each molecule's protein levels in VEGFR2-blocking treatment comparing to controls. Values represent averages and standard deviations of three to five tumors for each treatment arm from two independent experiments, and the red dotted line represents a value of 1 (no change of expression in treatment).

VEGF-A, several FGF family members, Ephrin-A1, and Angiopoietin-1 all showed a significant induction, ranging from 1.5-fold to almost 3-fold in the anti-VEGFR2-treated tumors. Expression of the receptors for these three families of proangiogenic factors was not appreciably changed by the treatment (Figure 5B). To determine whether these genes were being upregulated in the tumor cells or in the endothelial cells, we dissected tumors and separated the endothelial cell and tumor cell populations by fluorescence-activated cell sorting (FACS), as previously described (Bergers et al., 2003). Using mRNA prepared from these two FACS-purified cell populations, we evaluated the expression levels of the proangiogenic ligands and found that most were upregulated in the tumor cell population (VEGF-A, FGF1, FGF2, FGF7, FGF8, Ephrin-A1, and Angiopoietin-2) whereas a partially overlapping set was upregulated in the tumor endothelial cells (FGF1, FGF2, Ephrin-A1, and Angiopoietin-1 and -2) (Figure 5B). To substantiate the RNA analysis, we also assessed several of these factors at the protein level, using immunoblotting and an antibody array with an ELISA-based quantitative readout. As shown in Figure 5C, protein levels of total VEGF, VEGF-164, FGF2, and Angiopoietin-1 were increased in the VEGFR2-blocking treatment when compared to mock-treated controls, as revealed by the two complementary assays, consistent with the RNA analysis. We also assessed the relative expression of these angiogenic factors after 4 weeks of treatment, when revascularization had occurred. Interestingly, their expression remained elevated in the anti-VEGFR2-treated tumors compared to mock-treated controls (data not shown), despite the fact that acute hypoxia was no longer detectable. Thus, some mechanism serves to sustain elevated expression of these factors once activated by acute hypoxia; one possibility is that low-level hypoxia not detectable by pimonidazole persists in the rebounding tumors in the absence of VEGF signaling, maintaining elevated expression of the upregulated angiogenic factors.

Seeking to substantiate the hypothesis that hypoxia was affecting the tumor cells, triggering the observed changes in expression of these proangiogenic factors, we analyzed the response of cultured islet tumor cells to hypoxia in vitro. When the βTC3 cell line derived from RIP-Tag2 tumors (Efrat et al., 1988) was cultured under hypoxic conditions (2% oxygen, 5% CO_2), VEGF-A, FGF2, and Ephrin-A1 mRNAs were upregulated, from 1.5-fold to 2.5-fold (Figure 6). VEGF and FGF2 were further analyzed at the protein level with the ELISA-based antibody array, and as shown in Figure 6, both were upregulated, a result that was consistent with the mRNA results. FGF1 was not induced by hypoxia in the cultured cells, in contrast to the results in whole tumors or FACS-purified primary tumor cells (compare Figure 5B and Figure 6). We suspect that these differences are consequent to the cell culture conditions and/or the adaptation of the tumor cells to culture.

Blocking FGF signaling impairs the evasion of VEGFR2 inhibition

Collectively, the data suggest that phenotypic resistance to extended VEGFR2-blocking treatment results from a hypoxia-driven change in the repertoire of proangiogenic factors expressed, enabling a transition from primary dependence on VEGF signaling to reliance instead on alternative angiogenic factors. While the VEGF-A ligand is itself upregulated in the treated tumors (and hypoxic tumor cell lines), it is evidently in-

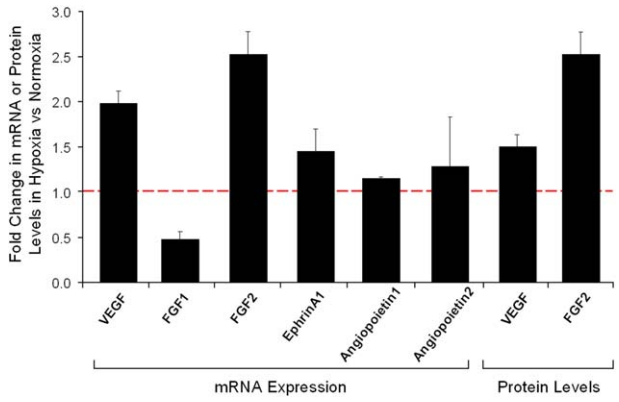

Figure 6. Hypoxia induces increased expression of proangiogenic factors in tumor-derived βTC cell lines

RIP-Tag2 tumor-derived cells (βTC3) were cultured in vitro under normoxic (20% oxygen, 5% CO_2) or hypoxic (2% oxygen, 5% CO_2) conditions for 24 hr, and quantitative RT-PCR analysis (mRNA Expression) and protein level analysis of several proangiogenic factors were performed as described in the Experimental Procedures section. Results are plotted as fold change in hypoxic versus normoxic culture conditions for each of the proangiogenic factors noted. Values represent averages and standard deviations of two independent experiments, and the red dotted line represents a value of 1 (no change of expression in treatment).

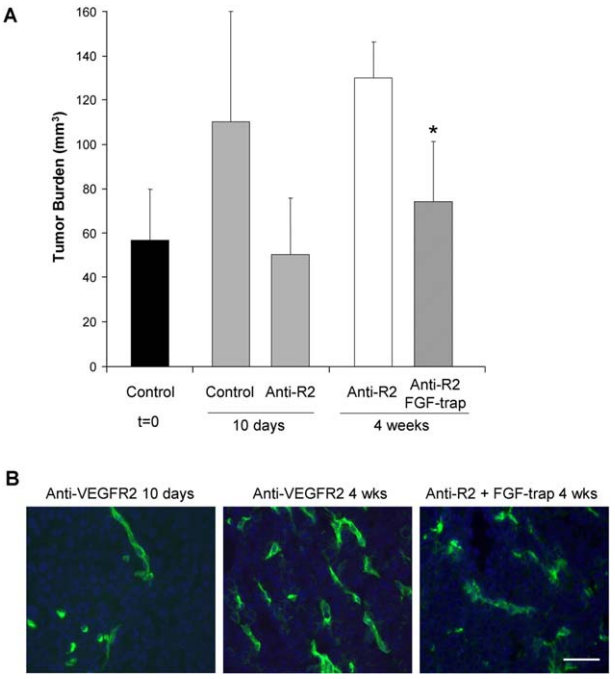

Figure 7. Proangiogenic ligands from the FGF family are important for reestablishing the vasculature and supporting regrowth of tumors

A: Quantification of overall tumor burden per animal for 10 days and 4 weeks of the different treatment groups, as noted. Averages from cohorts of eight to ten mice are plotted with their respective standard deviation bars. *Statistically significant differences using Mann-Whitney test ($p < 0.02$) when comparing anti-VEGFR2 + FGF-trap combination to anti-VEGFR2 alone.

B: Vessel labeling by FITC-conjugated tomato lectin (green) and DAPI counterstain of nuclei (blue) for the different time points and treatment arms as noted. Images shown are representative of an analysis of a minimum of five sections from each of eight animals from every treatment group; scale bar, 50 μm. Quantification of intratumoral vessel density revealed a 41% reduction of the vessel density in the dual anti-VEGFR2 + FGF-trap combination treatment, as compared to anti-VEGFR2 alone ($p = 0.02$, Mann-Whitney test).

effectual, due to the continuing blockade of VEGFR2 signaling (evidenced by the suppression of VEGFR2 phosphorylation; see Figures 4A and 4B). We postulated, therefore, that the hypoxia-triggered upregulation of other proangiogenic factors was the driving force in reactivating angiogenesis in the face of VEGFR2 blockade. To test this hypothesis, we designed a two-stage regression trial regimen, beginning with anti-VEGFR2-blocking antibody treatment for 10 days. Then, at +10 days (when efficacy of the monotherapy was maximal), we added on a blockade of the proangiogenic FGFs, using an adenovirus-delivered soluble form of FGFR2 (FGF-trap), seeking to inhibit revascularization and tumor progression. The FGF-trap adenovirus has been previously reported to bind and block various ligands of the FGF family, including FGF1, FGF3, FGF7, and FGF10, thereby effectively inhibiting angiogenesis in vitro and in vivo (Compagni et al., 2000). Indeed, adding the FGF-trap treatment in the regrowth phase produced a significant decrease in tumor growth compared to anti-VEGFR2 alone (Figure 7A). This decrease in tumor burden was accompanied by a decrease in angiogenesis that was observed as decreased intratumoral vessel density (Figure 7B). Quantification of this parameter revealed a 41% reduction of the vessel density in the dual anti-VEGFR2 + FGF-trap combination treatment, as compared to anti-VEGFR2 alone ($p = 0.02$, Mann-Whitney test). Histological analysis by H&E staining of the dual-treated tumors revealed a phenotype that was similar to that of tumors treated only with anti-VEGFR2-blocking antibody: the tumors were smaller but more locally invasive (data not shown). In sum, the data functionally implicate proangiogenic FGF ligands in the reestablishment of the vasculature and regrowth of tumors that manifest phenotypic resistance, and demonstrate that concomitant blockade of both VEGF and FGF signaling serves to limit the evasive reinduction of angiogenesis and consequent regrowth of the tumors. Although tumor burden and vessel density are significantly decreased in this double-targeted anti-VEGFR2 and FGF-trap treatment, both parameters are still slightly higher than the phase of maximal response to single VEGFR2 blockade (in Figure 7, compare anti-R2 at 10 days to anti-R2 + FGF-trap at 4 weeks), suggesting that other proangiogenic factors, e.g., Ephrins or Angiopoietins, could be additionally stimulating tumor angiogenesis and facilitating tumor growth.

Discussion

The studies reported herein with function-blocking monoclonal antibodies have revealed that VEGFR2 plays a critical role in promoting and sustaining angiogenesis in pancreatic islet cell tumors. The data further demonstrate that VEGFR2 blockade is an effective antiangiogenic and antitumor agent, whose effects are associated with decreased vessel density, decreased vascular permeability, and reduced microhemorrhaging. In marked contrast, although VEGFR1 is expressed in the premalignant and tumor stages in this model (Christofori et al., 1995; and data not shown), blocking VEGFR1 did not affect tumor

progression or angiogenesis in any of the trials performed. VEGFR1 has on the one hand been implicated by gene knockout studies as a nonsignaling "sink" or "depot" for VEGF ligand (Hiratsuka et al., 1998). More recently, however, this receptor has been implicated in other processes of potential importance for tumorigenesis, including macrophage mobilization (Sawano et al., 2001) and recruitment of hematopoietic stem cells to the neovessels of tumors (Hattori et al., 2002; Rabbany et al., 2003). In the RIP-Tag2 model of pancreatic islet carcinoma, innate immune cells have been documented to play an important role in supplying the tumor with metalloproteinases and other matrix-degrading enzymes that trigger angiogenesis and tumor progression (Bergers et al., 2000; Joyce et al., 2004, 2005). Our results indicate that macrophage recruitment is not affected by the blockade of VEGFR1 or VEGFR2 (data not shown), suggesting that other signaling molecules are promoting the innate immune infiltration. VEGFR1 has also been implicated in the recruitment of bone marrow-derived hematopoietic stem cells to the neovessels of tumors (Hattori et al., 2002; Rabbany et al., 2003). Our data, which indicate that blocking VEGFR1 does not alter the tumor progression or the angiogenic phenotype in the course of pancreatic islet carcinogenesis, suggest that this tumor type is not dependent on such hematopoietic precursors, consistent with other studies in which we have failed to document significant incorporation of marked bone marrow-derived cells into tumor vasculature (D. McDonald and D.H., unpublished data).

Drug resistance by circumventing VEGF receptor blockade

Although the VEGF-VEGFR2 signaling circuit is an increasingly validated target in solid tumors, eventual progression of disease in the face of VEGF/VEGFR therapies has been described in clinical trials and in mouse models of cancer (Broxterman et al., 2003; Kerbel et al., 2001; Miller et al., 2003, 2005; Klement et al., 2000). Our results of phenotypic resistance in extended regression trials with the VEGFR2-blocking treatment are consistent with these previous findings and further support the existence of mechanisms for phenotypic resistance or escape from the effects of anti-VEGFR treatment. Notably, we observe a period of stable disease followed by progression, accompanied by a significant life span extension. This pattern of tumor stasis and then tumor growth is arguably analogous to the delayed time to progression seen in the clinical trials with bevacizumab (Avastin) as monotherapy (Yang et al., 2003) or in combination with chemotherapy (Hurwitz et al., 2004). Furthermore, our results suggest a mechanism by which the tumors develop the capability to begin regrowing in the face of VEGFR2 blockade with restoration of high blood vessel density. This escape is not a failure in the VEGFR2 blockade, since the vessel microhemorrhaging and VEGFR2-activating phosphorylation are both comparably reduced at the short- and long-term treatments. Rather, the data implicate hypoxia-triggered upregulation other proangiogenic factors (FGFs and Ephrins) that restimulate tumor angiogenesis in a VEGF-independent fashion, as schematized in Figure 8. Indeed, our two-phase dual blockade of VEGFR2 and FGF ligands produced a significant inhibition of angiogenesis and tumor growth, demonstrating a role for FGF ligands in the late-phase evasion of anti-VEGFR2 treatment.

While the proangiogenic FGFs and Ephrins have been previously implicated in RIP-Tag2 angiogenesis (Brantley et al., 2002; Cheng et al., 2003; Compagni et al., 2000), they seem to play a supporting role to VEGF in the early stages of islet tumorigenesis. Both a tissue-specific gene knockout (Inoue et al., 2002) and pharmacological inhibition of VEGFR signaling with small molecule kinase inhibitors (Bergers et al., 2000, 2003) indicate that VEGF is crucial in the early stages of tumor progression, for angiogenic switching, tumor formation, and initial tumor growth. By contrast, VEGFR inhibition was equivocal when used as monotherapy against late-stage tumors (Bergers et al., 2003; and this study). Collectively the data suggest that these other proangiogenic circuits primarily serve to enhance the critical VEGFR signal in early-stage lesions, whereas in later stages of progression, they can either enhance VEGF signaling or indeed substitute for it. Thus, in the face of VEGFR2 inhibition, other proangiogenic factors can circumvent the blockade, to promote a new wave of angiogenesis and tumor growth. Interestingly, analysis of the revascularized VEGFR2-blocked tumors in the regrowth and progression phase after 4 weeks of treatment showed that, although acute hypoxia was no longer detectable with our assays, moderately increased expression of the proangiogenic factors persisted (data not shown). One attractive model, to be investigated in future studies, is that subtle hypoxia persists in the tumors whose growth and progression is supported by alternative tumor angiogenesis factors, thereby maintaining their elevated expression once activated in the acute hypoxic phase.

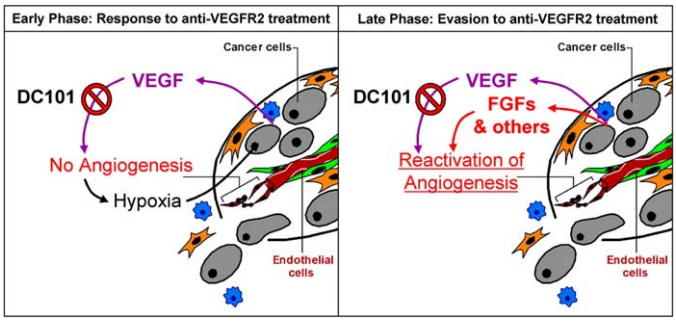

Figure 8. Model of the early and late phases of response to anti-VEGFR2 therapy in the RIP-Tag2 islet carcinogenesis model

Differential effects are apparent in the early-stage versus late-stage anti-VEGFR2 treatment. In the initial phase (left), VEGF is the main regulator of angiogenesis (purple arrows), and the VEGFR2 blockade causes vascular and tumoral regression (objective response). Nevertheless, it also causes regions of hypoxia (black arrows) in the tumors that initiate the circumvention phase. In this latter phase of circumvention (right), which produces phenotypic resistance to VEGFR2 blockade, the tumor cells upregulate expression of other proangiogenic factors, including FGFs (red arrows) that are demonstrably important in this model for the observed reactivation of angiogenesis. The result is reestablishment of the tumor vasculature and progression to continuing tumor growth.

Translational implications

We show, in a two-stage regression trial regimen, that adding an inhibitor of the circumventing FGF signal when the VEGF therapy is beginning to fail can significantly retard reinitiation of angiogenesis and tumor progression. To date, human clinical trials that selectively target VEGF or VEGFRs are merely delaying time to progression after a period of stable disease, thus

affording a modest survival advantage (e.g., Hurwitz et al., 2004), much like that seen in this mouse model of cancer. We imagine that similar mechanisms are operative in such human tumors whereby alternative proangiogenic signaling circuits are upregulated and come to supplant to varying degrees the dependence on VEGF. It will be of considerable interest to analyze biopsies from patients whose tumors are progressing in the face of VEGF/VEGFR blockade, to see whether this means of evasion is similarly operative. If so, we foresee two possible means to interfere with this phenotypic resistance to VEGF/VEGFR therapy in human cancer. First, inhibitors of the circumventing proangiogenic factors could be introduced into the trial regimens at the time of progression. Alternatively, multitargeted inhibitors, or cocktails of specific inhibitors (e.g., of VEGF, FGF, and likely Ephrins, etc.) could be used initially, seeking to keep the angiogenic switch shut off, avoiding the secondary wave of angiogenesis consequent to hypoxia-induced upregulation of alternative proangiogenic growth factors in the face of VEGF signaling inhibition. Much as knowledge of classical drug resistance mechanisms is providing rational inroads to finesse them, we suggest that insight into phenotypic resistance to VEGF/VEGFR-targeted therapy will afford means to develop antiangiogenic therapies with enduring efficacy.

Experimental procedures

Generation of RIP-Tag2;Rag1 knockout

The generation and characterization of the single transgenic RIP-Tag2 mice (Hanahan, 1985) and the Rag1 knockout (Mombaerts et al., 1992) have been previously reported. RIP-Tag2 inbred in C57-Bl6-J was crossed to $Rag1^{tm1Mom}$ C57-Bl6-J from Jackson Labs. As the two genes sit in close proximity in mouse chromosome 2, the screening of more than 100 pups was necessary until a recombinant chromosome RIP-Tag2;Rag1 null was obtained. This "founder" animal was backcrossed to Rag1 null animals to obtain RIP-Tag2;Rag1 null homozygotes. All housing, care, and experiments with mice were performed in accordance with the University of California, San Francisco (UCSF) institutional and national guidelines and regulations governing the care of laboratory mice.

Therapeutic antibody treatment

Rat monoclonal function-blocking antibodies against VEGFR1 (MF1) and VEGFR2 (DC101) were obtained from ImClone Systems Incorporated (New York, NY). The dosage regimen used was 1 mg DC101 per mouse and 1.25 mg MF1 per mouse twice a week through intraperitoneal injection. Control animals were treated with purified rat IgG (ChromPure rat IgG, Jackson Immunoresearch) at a dose of 1.25 mg per mouse twice a week. Cohorts of eight to ten mice were treated per each arm of the trial study, and each trial was repeated at least once.

Standard methods

Standard techniques for quantitating angiogenic islets and tumors (Parangi et al., 1996), assessing histopathology and vascular morphology (Inoue et al., 2002; Bergers et al., 2003, Joyce et al., 2004) and vascular permeability (Miles and Miles, 1952), isolating constituent cells from tumors (Bergers et al., 2003), and the matrigel plug angiogenesis bioassay (Passaniti et al., 1992), are presented in the Supplemental Data.

Protein analysis of tumors and βTC cell lines

Whole tumor samples or βTC3 cell line pellets were lysed in RIPA buffer containing a cocktail of protease inhibitors (Leupeptin, Aprotinin, and PMSF), followed by homogenization and clearing by centrifugation as described elsewhere. Total protein (50 μg) was resolved in SDS-PAGE gels, transferred onto PVDF membranes, and analyzed by Western blotting using the following antibodies: anti-VEGF Ab-3 (JH121, Neomarkers, Labvision Corp.) and anti-Angiopoietin-1/4 (sc9360, Santa Cruz Biotech). Protein level analysis was also performed using an ELISA-based commercial antibody array ("Raybio Mouse Angiogenesis Ab-Array"; M0319801, RayBiotech Inc.,) which allows for quantitative determination of protein levels of a variety of proangiogenic factors including total VEGF and FGF2. Hybridization and detection were performed following manufacturer's instructions using 500 μg of tumor lysates or βTC3 cell lysates. Western blot immunodetection of phospho-VEGFR2 was performed using a mouse anti-phospho-VEGFR2 Y951, clone 7H11 (#2467, Cell Signaling Technology) as described (Matsumoto et al., 2005) starting from 200 μg of tumor lysates. For all the Western blots and the antibody array, quantification of band or spot intensities was performed using BioRad Quantity One software.

Hypoxia assays

Hypoxia in islet tumors was detected by the formation of pimonidazole adducts after the injection of pimonidazole hydrochloride compound into tumor-bearing animals for 2 hr. Pancreas sections were immunostained to detect pimonidazole adducts using Hypoxyprobe-1-Mab1 antibody (Hypoxyprobe kit, Chemicon) following the manufacturer's instructions. For the hypoxia in culture, RIP-Tag2 tumor cells were cultured under normoxic (20% oxygen, 5% CO_2) or hypoxic (2% oxygen, 5% CO_2) conditions in a three-gases hypoxic chamber for 24 hr rapidly followed by lysis and RNA extraction (RNeasy, Qiagen) and TaqMan quantitative RT-PCR reaction as previously described.

FGF-trap preparation and therapy

Adenovirus FGF-trap was developed and described previously (Compagni et al., 2000), and preparation of high-titer adenovirus was subcontracted to Vector Biolabs, Philadelphia, PA. Adenovirus FGF-trap was tested in vitro for sFGFR2iiib production in HeLa cells and for FGF-driven proliferation in HUVEC cells as described (Compagni et al., 2000). In vivo delivery to RIP-Tag2 mice was performed in a one-time intravascular injection of 1–3 × 10^9 viral infective units per animal and checked for serum presence of sFGFR2iiib protein by heparin-Sepharose immunoprecipitation, as described in Compagni et al. (2000).

Supplemental data

The Supplemental Data include Supplemental Experimental Procedures and two supplemental figures and can be found with this article online at http://www.cancercell.org/cgi/content/full/8/4/299/DC1/.

Acknowledgments

We would like to thank Gerhard Christofori (Institute of Biochemistry and Genetics, University of Basel, Switzerland) for providing us the FGF-trap adenovirus used in this study, Emily Bergsland (Comprehensive Cancer Center, UCSF) for critical reading of the manuscript, and Lena Claesson-Welsh (Department of Genetics and Pathology, Uppsala University) for helpful suggestions. We are thankful to Dale Milfay for excellent technical support with the adenovirus work; Marina Vayner, Susan Cacacho, and Ehud Drori for technical support; and Bill Bowes for continuing encouragement. This research was supported by a joint grant from the US National Cancer Institute (to D.H. and G.B.) and the William F. Bowes, Jr. Foundation. D.H. is an American Cancer Society Research Professor and thanks the ACS for their support. D.J.H. is an employee of ImClone Systems, which produced the DC101 and MF1 function-blocking antibodies for the VEGF receptors.

Received: May 13, 2005
Revised: September 6, 2005
Accepted: September 23, 2005
Published: October 17, 2005

References

Adams, T.E., Alpert, S., and Hanahan, D. (1987). Non-tolerance and autoantibodies to a transgenic self antigen expressed in pancreatic β cells. Nature *325*, 223–228.

Bergers, G., Javaherian, K., Lo, K.M., Folkman, J., and Hanahan, D. (1999). Effects of angiogenesis inhibitors on multistage carcinogenesis in mice. Science *284*, 808–812.

Bergers, G., Brekken, R., McMahon, G., Vu, T.H., Itoh, T., Tamaki, K., Tanzawa, K., Thorpe, P., Itohara, S., Werb, Z., and Hanahan, D. (2000). Matrix metalloproteinase-9 triggers the angiogenic switch during carcinogenesis. Nat. Cell Biol. *2*, 737–744.

Bergers, G., Song, S., Meyer-Morse, N., Bergsland, E., and Hanahan, D. (2003). Benefits of targeting both pericytes and endothelial cells in the tumor vasculature with kinase inhibitors. J. Clin. Invest. *111*, 1287–1295.

Brantley, D.M., Cheng, N., Thompson, E.J., Lin, Q., Brekken, R.A., Thorpe, P.E., Muraoka, R.S., Cerretti, D.P., Pozzi, A., Jackson, D., et al. (2002). Soluble Eph A receptors inhibit tumor angiogenesis and progression in vivo. Oncogene *21*, 7011–7026.

Broxterman, H.J., Lankelma, J., and Hoekman, K. (2003). Resistance to cytotoxic and anti-angiogenic anticancer agents: similarities and differences. Drug Resist. Updat. *6*, 111–127.

Cheng, N., Brantley, D., Fang, W.B., Liu, H., Fanslow, W., Cerretti, D.P., Bussell, K.N., Reith, A., Jackson, D., and Chen, J. (2003). Inhibition of VEGF-dependent multistage carcinogenesis by soluble EphA receptors. Neoplasia *5*, 445–456.

Christofori, G., Naik, P., and Hanahan, D. (1995). Vascular endothelial growth factor and its receptors, flt-1 and flk-1, are expressed in normal pancreatic islets and throughout islet cell tumorigenesis. Mol. Endocrinol. *9*, 1760–1770.

Compagni, A., Wilgenbus, P., Impagnatiello, M.A., Cotten, M., and Christofori, G. (2000). Fibroblast growth factors are required for efficient tumor angiogenesis. Cancer Res. *60*, 7163–7169.

Daniel, D., Meyer-Morse, N., Bergsland, E.K., Dehne, K., Coussens, L.M., and Hanahan, D. (2003). Immune enhancement of skin carcinogenesis by CD4+ T cells. J. Exp. Med. *197*, 1017–1028.

Daniel, D., Chiu, C., Giraudo, E., Inoue, M., Mizzen, L.A., Chu, N.R., and Hanahan, D. (2005). CD4+ T cell-mediated antigen-specific immunotherapy in a mouse model of cervical cancer. Cancer Res. *65*, 2018–2025.

de Visser, K.E., Korets, L.V., and Coussens, L.M. (2005). De novo carcinogenesis promoted by chronic inflammation is B lymphocyte dependent. Cancer Cell *7*, 411–423.

Dougher-Vermazen, M., Hulmes, J.D., Bohlen, P., and Terman, B.I. (1994). Biological activity and phosphorylation sites of the bacterially expressed cytosolic domain of the KDR VEGF-receptor. Biochem. Biophys. Res. Commun. *205*, 728–738.

Efrat, S., Linde, S., Kofod, H., Spector, D., Delannoy, M., Grant, S., Hanahan, D., and Baekkeskov, S. (1988). β-cell lines derived from transgenic mice expressing a hybrid insulin gene-oncogene. Proc. Natl. Acad. Sci. USA *85*, 9037–9041.

Ferrara, N., Gerber, H.P., and LeCouter, J. (2003). The biology of VEGF and its receptors. Nat. Med. *9*, 669–676.

Hanahan, D. (1985). Heritable formation of pancreatic β-cell tumours in transgenic mice expressing recombinant insulin/simian virus 40 oncogenes. Nature *315*, 115–122.

Hanahan, D., and Folkman, J. (1996). Patterns and emerging mechanisms of the angiogenic switch during tumorigenesis. Cell *86*, 353–364.

Hattori, K., Heissig, B., Wu, Y., Dias, S., Tejada, R., Ferris, B., Hicklin, D.J., Zhu, Z., Bohlen, P., Witte, L., et al. (2002). Placental growth factor reconstitutes hematopoiesis by recruiting VEGFR1(+) stem cells from bone-marrow microenvironment. Nat. Med. *8*, 841–849.

Hiratsuka, S., Minowa, O., Kuno, J., Noda, T., and Shibuya, M. (1998). Flt-1 lacking the tyrosine kinase domain is sufficient for normal development and angiogenesis in mice. Proc. Natl. Acad. Sci. USA *95*, 9349–9354.

Holash, J., Maisonpierre, P.C., Compton, D., Boland, P., Alexander, C.R., Zagzag, D., Yancopoulos, G.D., and Wiegand, S.J. (1999). Vessel cooption, regression, and growth in tumors mediated by angiopoietins and VEGF. Science *284*, 1994–1998.

Hurwitz, H., Fehrenbacher, L., Novotny, W., Cartwright, T., Hainsworth, J., Heim, W., Berlin, J., Baron, A., Griffing, S., Holmgren, E., et al. (2004). Bevacizumab plus irinotecan, fluorouracil, and leucovorin for metastatic colorectal cancer. N. Engl. J. Med. *350*, 2335–2342.

Inoue, M., Hager, J.H., Ferrara, N., Gerber, H.P., and Hanahan, D. (2002). VEGF-A has a critical, nonredundant role in angiogenic switching and pancreatic β cell carcinogenesis. Cancer Cell *1*, 193–202.

Jolicoeur, C., Hanahan, D., and Smith, K. (1994). T cell tolerance towards a transgenic β cell antigen and transcription of endogenous pancreatic genes in the thymus. Proc. Natl. Acad. Sci. USA *91*, 6707–6711.

Joyce, J.A., Baruch, A., Chehade, K., Meyer-Morse, N., Giraudo, E., Tsai, F.Y., Greenbaum, D.C., Hager, J.H., Bogyo, M., and Hanahan, D. (2004). Cathepsin cysteine proteases are effectors of invasive growth and angiogenesis during multistage tumorigenesis. Cancer Cell *5*, 443–453.

Joyce, J.A., Freeman, C., Meyer-Morse, N., Parish, C.R., and Hanahan, D. (2005). A functional heparan sulfate mimetic implicates both heparanase and heparan sulfate in tumor angiogenesis and invasion in a mouse model of multistage cancer. Oncogene *24*, 4037–4051.

Kerbel, R.S., Yu, J., Tran, J., Man, S., Viloria-Petit, A., Klement, G., Coomber, B.L., and Rak, J. (2001). Possible mechanisms of acquired resistance to anti-angiogenic drugs: implications for the use of combination therapy approaches. Cancer Metastasis Rev. *20*, 79–86.

Klement, G., Baruchel, S., Rak, J., Man, S., Clark, K., Hicklin, D.J., Bohlen, P., and Kerbel, R.S. (2000). Continuous low-dose therapy with vinblastine and VEGF receptor-2 antibody induces sustained tumor regression without overt toxicity. J. Clin. Invest. *105*, R15–R24.

Leenders, W.P., Kusters, B., Verrijp, K., Maass, C., Wesseling, P., Heerschap, A., Ruiter, D., Ryan, A., and de Waal, R. (2004). Antiangiogenic therapy of cerebral melanoma metastases results in sustained tumor progression via vessel co-option. Clin. Cancer Res. *10*, 6222–6230.

Luttun, A., Tjwa, M., Moons, L., Wu, Y., Angelillo-Scherrer, A., Liao, F., Nagy, J.A., Hooper, A., Priller, J., De Klerck, B., et al. (2002). Revascularization of ischemic tissues by PlGF treatment, and inhibition of tumor angiogenesis, arthritis and atherosclerosis by anti-Flt1. Nat. Med. *8*, 831–840.

Matsumoto, T., Bohman, S., Dixelius, J., Berge, T., Dimberg, A., Magnusson, P., Wang, L., Wikner, C., Qi, J.H., Wernstedt, C., et al. (2005). VEGF receptor-2 Y951 signaling and a role for the adapter molecule TSAd in tumor angiogenesis. EMBO J. *24*, 2342–2353.

Miles, A.A., and Miles, E.M. (1952). Vascular reactions to histamine, histamine-liberator and leukotaxine in the skin of guinea-pigs. J. Physiol. *118*, 228–257.

Miller, K.D., Sweeney, C.J., and Sledge, G.W., Jr. (2003). The Snark is a Boojum: the continuing problem of drug resistance in the antiangiogenic era. Ann. Oncol. *14*, 20–28.

Miller, K.D., Sweeney, C.J., and Sledge, G.W., Jr. (2005). Can tumor angiogenesis be inhibited without resistance? EXS *94*, 95–112.

Mombaerts, P., Iacomini, J., Johnson, R.S., Herrup, K., Tonegawa, S., and Papaioannou, V.E. (1992). RAG-1-deficient mice have no mature B and T lymphocytes. Cell *68*, 869–877.

Parangi, S., O'Reilly, M., Christofori, G., Holmgren, L., Grosfeld, J., Folkman, J., and Hanahan, D. (1996). Antiangiogenic therapy of transgenic mice impairs de novo tumor growth. Proc. Natl. Acad. Sci. USA *93*, 2002–2007.

Passaniti, A., Taylor, R.M., Pili, R., Guo, Y., Long, P.V., Haney, J.A., Pauly, R.R., Grant, D.S., and Martin, G.R. (1992). A simple, quantitative method for assessing angiogenesis and antiangiogenic agents using reconstituted basement membrane, heparin, and fibroblast growth factor. Lab. Invest. *67*, 519–528.

Pennacchietti, S., Michieli, P., Galluzzo, M., Mazzone, M., Giordano, S., and Comoglio, P.M. (2003). Hypoxia promotes invasive growth by transcriptional activation of the met protooncogene. Cancer Cell *3*, 347–361.

Pezzella, F., Pastorino, U., Tagliabue, E., Andreola, S., Sozzi, G., Gasparini, G., Menard, S., Gatter, K.C., Harris, A.L., Fox, S., et al. (1997). Non-small-cell lung carcinoma tumor growth without morphological evidence of neoangiogenesis. Am. J. Pathol. *151*, 1417–1423.

Pugh, C.W., and Ratcliffe, P.J. (2003). Regulation of angiogenesis by hypoxia: role of the HIF system. Nat. Med. *9*, 677–684.

Rabbany, S.Y., Heissig, B., Hattori, K., and Rafii, S. (2003). Molecular pathways regulating mobilization of marrow-derived stem cells for tissue revascularization. Trends Mol. Med. *9*, 109–117.

Ryschich, E., Schmidt, J., Hammerling, G.J., Klar, E., and Ganss, R. (2002). Transformation of the microvascular system during multistage tumorigenesis. Int. J. Cancer *97*, 719–725.

Sawano, A., Iwai, S., Sakurai, Y., Ito, M., Shitara, K., Nakahata, T., and Shibuya, M. (2001). Flt-1, vascular endothelial growth factor receptor 1, is a novel cell surface marker for the lineage of monocyte-macrophages in humans. Blood *97*, 785–791.

Shibuya, M. (2001). Structure and function of VEGF/VEGF-receptor system involved in angiogenesis. Cell Struct. Funct. *26*, 25–35.

Steeg, P.S. (2003). Angiogenesis inhibitors: motivators of metastasis? Nat. Med. *9*, 822–823.

Yang, J.C., Haworth, L., Sherry, R.M., Hwu, P., Schwartzentruber, D.J., Topalian, S.L., Steinberg, S.M., Chen, H.X., and Rosenberg, S.A. (2003). A randomized trial of bevacizumab, an anti-vascular endothelial growth factor antibody, for metastatic renal cancer. N. Engl. J. Med. *349*, 427–434.

Yu, J.L., Rak, J.W., Coomber, B.L., Hicklin, D.J., and Kerbel, R.S. (2002). Effect of p53 status on tumor response to antiangiogenic therapy. Science *295*, 1526–1528.